Dynamic changes in the mobility of LAT in aggregated lipid rafts upon T cell activation

Natsuko Tanimura,[1] Masakazu Nagafuku,[1] Yasuko Minaki,[1] Yukio Umeda,[3] Fumie Hayashi,[1] Junko Sakakura,[1] Akiko Kato,[1] Douglas R. Liddicoat,[1] Masato Ogata,[2] Toshiyuki Hamaoka,[2] and Atsushi Kosugi[1,4]

[1]School of Allied Health Sciences, Faculty of Medicine, and [2]Department of Oncogenesis, Graduate School of Medicine (C6), Osaka University, Suita, Osaka 565-0871, Japan
[3]First Department of Surgery, Gifu University School of Medicine, Gifu, 500-8705, Japan
[4]Core Research for Evaluational Science and Technology program (CREST), Japan Science and Technology Corporation (JST), Saitama, 332-0012 Japan

Lipid rafts are known to aggregate in response to various stimuli. By way of raft aggregation after stimulation, signaling molecules in rafts accumulate and interact so that the signal received at a given membrane receptor is amplified efficiently from the site of aggregation. To elucidate the process of lipid raft aggregation during T cell activation, we analyzed the dynamic changes of a raft-associated protein, linker for activation of T cells (LAT), on T cell receptor stimulation using LAT fused to GFP (LAT-GFP). When transfectants expressing LAT-GFP were stimulated with anti-CD3–coated beads, LAT-GFP aggregated and formed patches at the area of bead contact. Photobleaching experiments using live cells revealed that LAT-GFP in patches was markedly less mobile than that in nonpatched regions. The decreased mobility in patches was dependent on raft organization supported by membrane cholesterol and signaling molecule binding sites, especially the phospholipase Cγ1 binding site in the cytoplasmic domain of LAT. Thus, although LAT normally moves rapidly at the plasma membrane, it loses its mobility and becomes stably associated with aggregated rafts to ensure organized and sustained signal transduction required for T cell activation.

Introduction

T cell activation commences with the recognition of antigen by way of the T cell receptor (TCR),* which is expressed on the surface of T cells. Ligation of the TCR leads to a rapid rise in intracellular protein tyrosine phosphorylation, followed by a series of biochemical events that eventually result in gene expression and effector function (Weiss and Littman, 1994; Wange and Samelson, 1996). Recently, specialized subdomains of the plasma membrane known as lipid rafts, consisting of concentrated amounts of sphingolipids and cholesterol, have been shown to play important roles in early signal transduction in lymphocytes (Simons and Ikonen, 1997; Cherukuri et al., 2001; van der Goot and Harder, 2001). The existence of lipid rafts on T cell membranes and

their role as platforms for conducting TCR signal transduction is already well documented (Montixi et al., 1998; Moran and Miceli, 1998; Xavier et al., 1998; Janes et al., 1999; Viola et al., 1999; Boerth et al., 2000; Kosugi et al., 2001).

Linker for activation of T cells (LAT) is an adaptor protein that performs a critical function in raft-mediated TCR signal transduction (Zhang et al., 1998a,b). LAT localizes to the plasma membrane by way of its transmembrane domain, and by palmitoylation of two Cys residues in its juxtamembrane region, it localizes to rafts in the plasma membrane (Zhang et al., 1998b). In LAT-negative T cell lines, TCR signaling is severely impaired and cannot be reconstituted by transfection with LAT mutated at residues required for raft localization, effectively demonstrating that not only LAT expression, but also localization of this molecule to rafts is essential for TCR signaling (Finco et al., 1998; Zhang et al., 1999). After TCR engagement, LAT is tyrosine-phosphorylated by ZAP-70, creating docking sites for SH2 domain–containing effector proteins. Proteins that associate directly or indirectly with LAT include phospholipase Cγ1 (PLCγ1), phosphoinositide 3-kinase, Grb2, Gads, Cbl, Vav, Itk, and SLP-76 (Zhang et al., 1998a, 2000; Shan and Wange, 1999). By binding with these molecules, LAT activates a series of signaling reactions including PLCγ1/Ca²⁺ and Ras/MAPK pathways.

After TCR stimulation, rafts are thought to aggregate to mediate binding between raft-localized phosphorylated LAT and various other signaling molecules. Although rafts on live cells normally have a diameter of $\sim$70 nm or less (Varma and Mayor, 1998), after stimulation they aggregate with one another to become a larger size, and are observable under light microscopes. By way of raft aggregation after stimulation, signaling molecules in rafts accumulate and interact so that the signal received at the membrane receptor is amplified efficiently from the site of aggregation to the inside of the cell. Thus, raft aggregation is considered to be important for raft-mediated signaling pathways (Janes et al., 2000; van der Goot and Harder, 2001). It has already been shown that raft aggregation after stimulation is observed in T cells (Janes et al., 1999; Khan et al., 2001). However, the precise role of raft aggregation in T cell activation is presently unknown. It may be required for only the initial steps of signaling that induce interaction between LAT and other signaling molecules, leaving the progression of signaling further downstream to be predominantly performed by protein–protein interactions. Alternatively, poststimulatory raft aggregation may be required until an entire series of initial signals from the membrane are completed. Additionally, there has also been little investigation of any real-time kinetic change in LAT or other raft-localized proteins that may exist in aggregated rafts of individual living cells after TCR stimulation.

In this work, we have created a fusion protein of GFP connected to the COOH-terminal of LAT to investigate kinetic changes in LAT accumulated in aggregated rafts using fluorescence imaging. Here, we show that LAT present at sites of raft aggregation after TCR stimulation has mobility lower than that of LAT found in other areas of the plasma membrane. Moreover, we found that both raft structure and signaling molecule binding sites, especially the PLCγ1 binding site in the cytoplasmic domain of LAT, are important for maintenance of this reduction in LAT mobility in aggregated rafts.

Results

The LAT-GFP fusion protein localizes to rafts and is phosphorylated after TCR stimulation

A fusion gene was constructed consisting of GFP linked to the COOH-terminal of the entire LAT gene coding sequence. The LAT-GFP fusion gene was then transfected into Jurkat cells and stable transfectants were established. Previously, it has been shown that LAT localizes to rafts by way of palmitoylation of two Cys residues in its juxtamembrane region (Zhang et al., 1998b). To investigate whether LAT-GFP localized to rafts as per endogenous LAT, LAT-GFP transfectants were solubilized and the raft fraction was purified using a sucrose gradient. As shown in Fig. 1 A, LAT-GFP predominantly exists in rafts like endogenous LAT, suggesting that the fusion of GFP to LAT does not affect the localization of LAT in the plasma membrane.

Next, we investigated whether the LAT-GFP fusion protein was functioning as a signaling molecule. After stimulation of LAT-GFP transfectants with OKT3, LAT-GFP was found to be effectively phosphorylated (Fig. 1 B). We also observed that phosphorylation of LAT-GFP after TCR
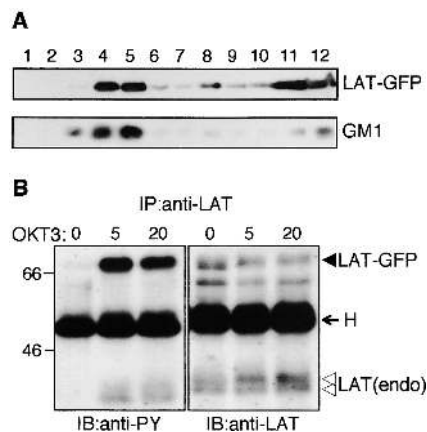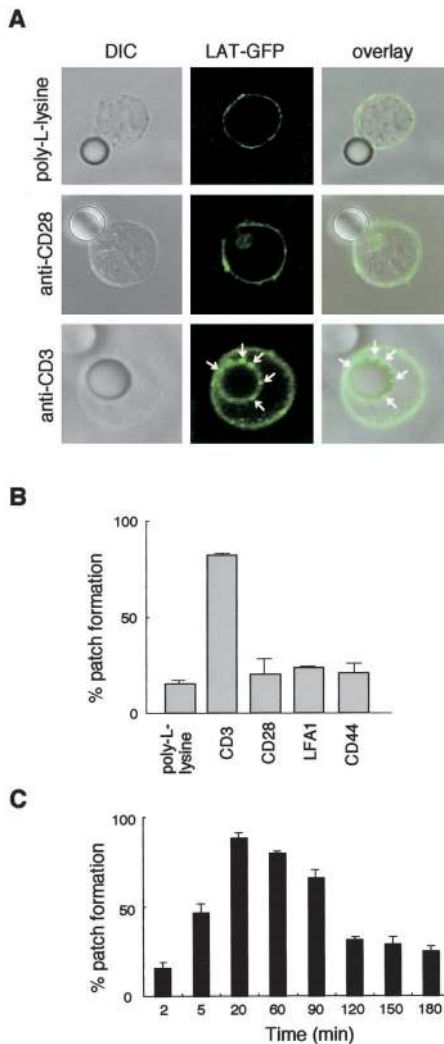

Figure 1. **Characterization of the LAT-GFP fusion protein used in this work.** (A) Localization of LAT-GFP in rafts from LAT-GFP–transfected Jurkat cells. LAT-GFP transfectants were lysed with MBS containing 1% Triton X-100, and the lysates were subjected to equilibrium gradient centrifugation. An aliquot of each fraction was electrophoresed and immunoblotted with HRP-conjugated CTx-B and anti-GFP antibody to detect GM1 and LAT-GFP, respectively. Fractions 4 and 5 correspond to the raft fractions. (B) Tyrosine phosphorylation of LAT-GFP after TCR cross-linking. The LAT-GFP transfectants were stimulated with OKT3 for the times indicated. Cell lysates were immunoprecipitated with anti-LAT antibody, and immunoprecipitates were analyzed by immunoblotting with anti-PY and anti-LAT antibodies. The closed arrowhead indicates LAT-GFP, whereas open arrowheads indicate endogenous LAT. The band migrating at 55 kD in each lane is the heavy chain (H) of the antibody used for immunoprecipitation.

stimulation mainly occurred in the raft fraction (unpublished data). These results strongly suggest that phosphorylated LAT-GFP could also function as an adaptor molecule after TCR engagement in LAT-GFP transfectants.

LAT-GFP patches form after T cell contact with anti-CD3–coated beads

Next, we investigated changes in the localization of LAT-GFP after TCR stimulation using confocal microscopy. LAT-GFP transfectants were stimulated with anti-CD3 antibody–coated latex beads, which have previously been reported to act as artificial antigen-presenting cells owing to their ability to induce cell polarization and reorganization of the cytoskeleton in Jurkat cells (Lowin-Kropf et al., 1998). After mixing LAT-GFP transfectants and the beads, these conjugates were fixed and LAT-GFP fluorescence was analyzed microscopically. Although LAT-GFP was homogeneously distributed at the plasma membrane in unstimulated cells, it became concentrated in distinct patches at the cell–bead interface in a large proportion of cells stimulated by the anti-CD3–coated beads (Fig. 2, A and B). When LAT-GFP transfectants were stimulated with poly-L-lysine–coated beads as a negative control, no patch formation was observed at the cell–bead interface.

To determine whether LAT-GFP patch formation was specifically induced by TCR cross-linking, antibodies directed against a variety of T cell surface molecules were bound to latex beads and used to stimulate LAT-GFP transfectants. All surface molecules analyzed were expressed at comparable levels between Jurkat cells and the transfectants
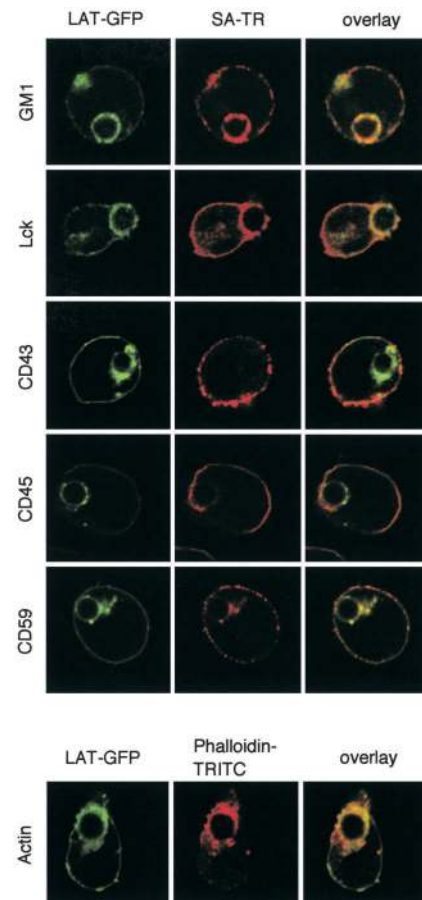
Next, we analyzed the kinetics of LAT-GFP patch formation after stimulation with anti-CD3–coated beads. The number of cell–bead conjugates with LAT-GFP patches increased from 5 min, peaked at 20 min, and continued to be observed until 90 min from time of initial stimulation. At 20 min after stimulation, anti-CD3–coated beads were mostly surrounded by the T cell surface and internalized (Fig. 2 A). Large decreases in the amount of patch formation were observed from 2 h after stimulation, suggesting that patch formation continues for ~90 min (Fig. 2 C).

Colocalization of raft markers to LAT-GFP patches

To determine whether sites of LAT-GFP patch formation corresponded with sites of raft aggregation, colocalization of molecules previously reported as raft markers to LAT-GFP patches was examined. Cholera toxin B (CTx-B) specifically binds to glycosphingolipids with a strong affinity for ganglioside GM1 (GM1), which is enriched in membrane rafts.

Figure 2. **TCR-mediated patch formation of LAT-GFP.** (A) LAT-GFP transfectants were mixed at a 2:1 ratio with poly-L-lysine–, anti-CD28–, or anti-CD3–coated latex beads. After 20 min at 37°C, conjugates were fixed with formaldehyde and observed by confocal microscopy. In the left column are bright-field images, in the middle column are LAT-GFP fluorescence images, and the right column contains the merged image of left and middle. LAT-GFP patches at the contact site between the cell and the bead are indicated by arrows. (B) Patch formation of LAT-GFP is specifically induced by TCR/CD3 cross-linking. LAT-GFP transfectants were mixed for 20 min with beads coated with either poly-L-lysine or antibodies against CD3, CD28, LFA-1, or CD44. Each column represents the average of at least three individual experiments in which more than 100 conjugates were scored for patch formation. Cells that incorporated or attached to beads were scored as conjugates. Cells that showed at least one distinct patch at the bead contact site were scored as positive for patch formation. (C) LAT-GFP transfectants were mixed with anti-CD3 beads at 37°C for the times indicated. Each column represents the average of at least three individual experiments.

Figure 3. **Colocalization of raft markers with LAT-GFP at the site of patch formation.** LAT-GFP transfectants were mixed with anti-CD3 beads for 20 min. Conjugates were fixed with formaldehyde, permeabilized, and stained with biotinylated CTx-B to detect GM1 or biotinylated anti-Lck, followed by incubation with SA-TR or with phalloidin-TRITC to detect F-actin. With regard to the staining for CD43, CD45, and CD59, conjugates were stained with biotinylated antibodies against CD43, CD45, and CD59 without permeabilization, followed by incubation with SA-TR, and were then fixed. Conjugates were observed by confocal microscopy. Single confocal sections show fluorescence in GFP and Texas red channels.

(unpublished data). Stimulation with anti-CD28 antibody–coated beads resulted in a lack of patch formation similar to that observed for poly-L-lysine beads (Fig. 2, A and B). Little patch formation was also observed when using beads conjugated to antibodies against LFA-1 and CD44 (Fig. 2 B). These results clearly demonstrate that LAT-GFP patch formation is specifically induced by TCR stimulation.

Figure 4. **LAT-GFP localized in patches is less mobile than that in nonpatched regions of the plasma membrane.** (A) After LAT-GFP transfectants were mixed with anti-CD3 beads for 20 min, a selected area (2-μm square) on the LAT-GFP patches or LAT-GFP in the plasma membrane (PM) was photobleached, and fluorescence recovery was monitored. Images at representative time points are shown. (B) Bleaching recovery kinetics is represented as the percentage of FRAP for LAT-GFP in patches and that in the plasma membrane. Data are representative of five individual experiments.
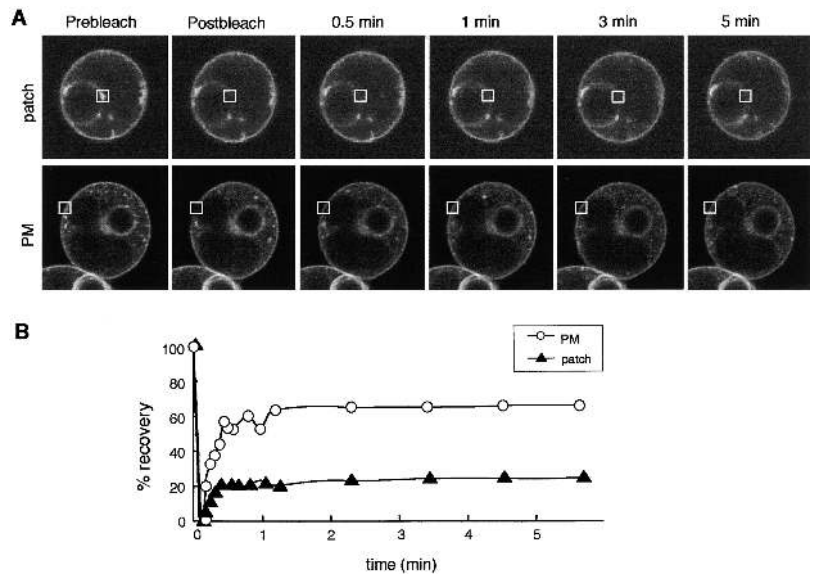
Hence, CTx-B was used to test whether GM1 colocalized with LAT-GFP patch sites. In addition to GM1, the expression pattern of CD59, CD45, CD43, Lck, and F-actin was also investigated. As shown in Fig. 3, GM1 and Lck were found to clearly colocalize with LAT-GFP patches. In addition, we observed an accumulation of F-actin in LAT-GFP patches. Previously, it was reported that raft patches formed by CD59 and GM1 accumulate F-actin (Harder and Simons, 1999). In contrast, CD43 and CD45, large glycoproteins that have been shown to be excluded from rafts (Rodgers and Rose, 1996; Janes et al., 1999; Allenspach et al., 2001), were mostly not colocalized with LAT-GFP patches. Although CD43 was distributed away from the cell–bead contact site, CD45 was partially expressed on the plasma membrane surrounding the beads. CD59, a glycosylphosphatidylinositol-anchored protein, could be used as another raft marker. CD59 formed patches not only at the bead interface, but also at the plasma membrane outside the cell–bead contact site in response to stimulation with anti-CD3–coated beads. In most cells, CD59 patches at the bead interface were colocalized with LAT-GFP patches as shown in Fig. 3, but there existed a certain number of cells that did not accumulate CD59 at the site of stimulation (unpublished data). Together, these results indicate that LAT-GFP patches have characteristics specific for aggregated lipid rafts.

LAT-GFP in patches is less mobile than that in nonpatch regions of the plasma membrane

Next, we analyzed the change in mobility of LAT-GFP in live cells using the FRAP technique. After stimulation of LAT-GFP transfectants with anti-CD3–coated beads, a single photobleach was applied to areas of patch formation and the fluorescence recovery into these bleached regions was monitored. As shown in Fig. 4 A, fluorescence in a LAT-GFP patch was completely lost immediately after photobleaching, and little recovery was observed even 5 min after photobleaching. It should be noted that another LAT-GFP patch just below the bleached area was constantly observed during this experiment. This excludes the possibility

that lack of fluorescence recovery in the bleached region was due to a movement of the cell, by itself. In contrast to LAT-GFP in patch areas, fluorescence of LAT-GFP in the plasma membrane outside the cell–bead interface was quickly recovered (Fig. 4 A). Whether we photobleached patch areas or the plasma membrane (nonpatch) areas, fluorescence recovered to a plateau level between 1 to 2 min after the initial bleach. However, although LAT-GFP fluorescence in the nonpatch area returned to ∼70% of total fluorescence, recovery in patch areas was limited to only 20% (Fig. 4 B). The recovery of LAT-GFP fluorescence in the plasma membrane from cells without stimulation was almost equivalent to that seen for bleaching of the plasma membrane from cells with bead stimulation (unpublished data). These results suggest that LAT localized in areas of raft aggregation has a remarkably low mobility compared with that in the plasma membrane outside aggregated rafts. LAT that does not accumulate in aggregated rafts maintains its rapid mobility irrespective of TCR stimulation.

The mobility of LAT-GFP in patches in primary activated T cells

Because dynamics of LAT after T cell activation could be different in primary T cells compared with that in Jurkat cells, we next investigated the mobility of LAT-GFP in primary activated T cells. C57BL/6 T cells were activated with anti-CD3 plus anti-CD28 and transduced with retrovirus encoding LAT-GFP. These cells were stimulated with antibody-coated beads and LAT-GFP fluorescence was analyzed. Because a previous report demonstrated that raft aggregation was greatly influenced by costimulatory signal in primary resting T cells (Viola et al., 1999), we compared the efficiency of patch formation in cells stimulated with beads coated with anti-TCR alone or with anti-TCR plus anti-CD28. As shown in Fig. 5 (A and B), LAT-GFP patches similar to that observed in Jurkat-derived transfectants were clearly detectable when cells were stimulated with anti-TCR plus anti-CD28 beads. Although stimulation for primary T cells with anti-TCR beads alone was able to induce LAT-
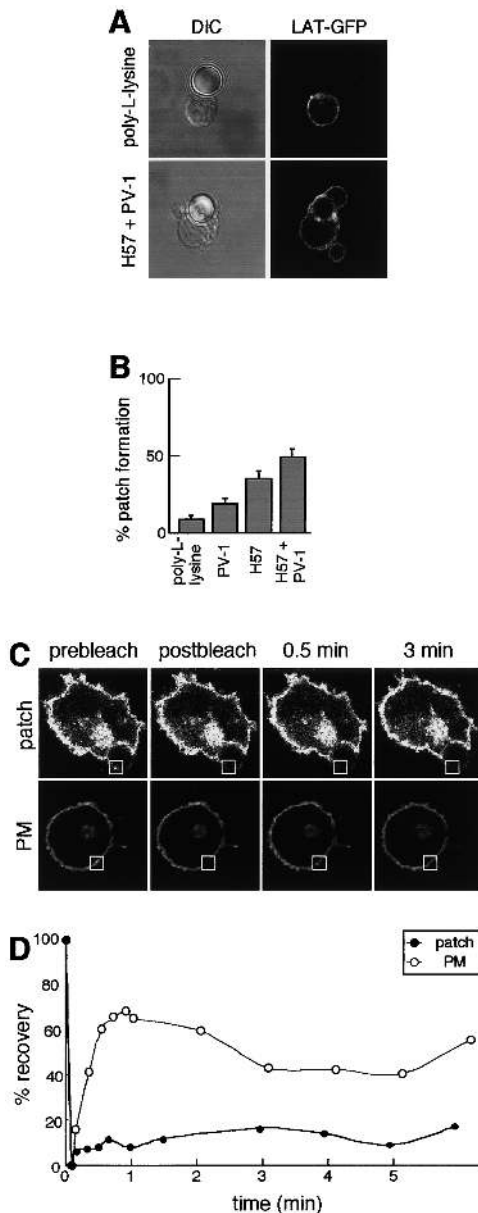
Figure 5. The mobility of LAT-GFP in patches in primary activated T cells. Primary activated T cells transduced with LAT-GFP were stimulated with antibody-coated beads and LAT-GFP fluorescence was analyzed. (A and B) Primary activated T cells were stimulated with poly-L-lysine–, anti-CD28 (PV1)–, anti-TCRβ (H57)–, or anti-TCRβ plus anti-CD28 (H57+PV-1)–coated beads. After 20 min at 37°C, conjugates were fixed with formaldehyde and observed by confocal microscopy. In the left column are differential interference contrast (DIC) images, and in the left column are LAT-GFP fluorescence images. Each column represents the average of at least three individual experiments in which more than 100 conjugates were scored for patch formation. (C) A selected area (2-μm square) on the LAT-GFP patches or LAT-GFP in the plasma membrane (PM) was photobleached, and fluorescence recovery was monitored. Images at representative time points are shown. (D) Bleaching recovery kinetics is represented as the percentage of FRAP for LAT-GFP in patches and that in the plasma membrane. Data are representative of three individual experiments.

GFP patches qualitatively similar to those observed in anti-TCR plus anti-CD28 bead stimulation, the frequency of patch formation was clearly reduced (Fig. 5 B). This suggests
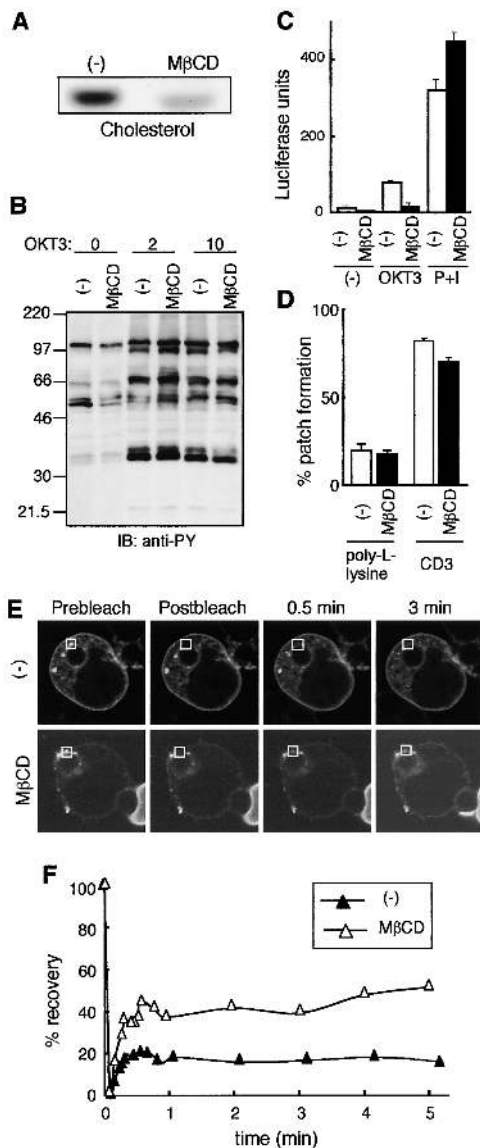
that the requirements for activation of raft aggregation are different in Jurkat and primary activated T cells.

The results obtained by FRAP experiments using live primary T cells were almost identical to those in Jurkat-derived transfectants. Although the recovery of LAT-GFP fluorescence in the nonpatch area of the plasma membrane reached 50% (Fig. 5, C and D). This result strongly argues that LAT mobility is generally reduced in the aggregated rafts of activated T cells.

Effects of cholesterol depletion on the mobility of LAT-GFP

Next, we wanted to determine the effect of cholesterol depletion on the mobility of LAT-GFP after TCR stimulation. To this end, we used methyl-β-cyclodextrin (MβCD), a reagent that selectively binds and removes cholesterol from the plasma membrane (Klein et al., 1995). Because extraction with 10 mM MβCD for longer than 20 min resulted in significant cell death due to the strong toxicity (unpublished data), we reduced the concentration of MβCD to 4 mM. It was reported that Jurkat cells can be viably cultured for 40 min or more while reducing cholesterol levels to ~50% with this concentration (Harder and Kuhn, 2000), and we confirmed a similar reduction in cholesterol by lipid analysis using high performance thin layer chromatography (HPTLC; Fig. 6 A). When we analyzed tyrosine phosphorylation of intracellular proteins after TCR stimulation in Jurkat cells treated for 40 min with 4 mM MβCD, we found no significant inhibition in this response (Fig. 6 B). Tyrosine phosphorylation of intracellular proteins and an increase of intracellular Ca^{2+} (unpublished data) were both clearly induced in response to TCR stimulation in Jurkat cells extracted under this condition, suggesting that extraction with 4 mM MβCD for 40 min does not affect early signaling events after TCR stimulation. However, we observed a clear inhibition of late signaling events with this treatment. Because prolonged treatments with MβCD significantly reduced cell viability even at a concentration of 4 mM, we analyzed the induction of NFAT transcription factor in MβCD-treated cells with the following protocol: Jurkat cells were transiently transfected with an NFAT-luc reporter plasmid; treated with MβCD for 40 min; washed; stimulated with OKT3 or PMA plus ionomycin in conditioned culture medium without FCS for 6 h; and tested for NFAT activity. In this assay, we observed a significant reduction in TCR-mediated NFAT activation by MβCD treatment without detriment to cell viability and recovery (Fig. 6 C). Culturing MβCD-treated Jurkat cells in medium containing 10% FCS completely cancelled the inhibition NFAT activity, presumably due to incorporation of exogenous cholesterol in FCS into cells (unpublished data). Together, extraction with 4 mM MβCD for 40 min seemed to impair late signaling events without affecting early signaling events after TCR stimulation.

After culturing LAT-GFP transfectants for 40 min in 4 mM MβCD, the cells were stimulated with anti-CD3–coated beads in the presence of 4 mM MβCD for 20 min. The effect of this treatment was then observed by confocal microscopy. LAT-GFP patches were clearly observed at the interface between cells and beads, and there was no signifi-

A

(-)   MβCD

Cholesterol

B

OKT3: 0   2   10

220
97
66
46
30
21.5

IB: anti-PY

C

Luciferase units

400

200

(-) MβCD (-) MβCD (-) MβCD
(-)   OKT3   P+I

D

% patch formation

100

50

(-) MβCD   (-) MβCD
poly-L-
lysine   CD3

E

	Prebleach	Postbleach	0.5 min	3 min
(-)				
MβCD				

F

% recovery

100
80
60
40
20
0

(-)
MβCD

0   1   2   3   4   5
time (min)

Figure 6.   The effect of cholesterol depletion on the mobility of LAT-GFP in patches. (A) Cholesterol in Jurkat cells treated with or without 4 mM MβCD for 40 min was extracted, separated with HPTLC, and visualized with 3% cupric acetate/8% phosphoric acid. (B) Jurkat cells treated with or without MβCD were stimulated with OKT3 for the times indicated. Tyrosine phosphorylation of cellular proteins was analyzed by immunoblotting using anti-PY antibody. (C) Jurkat cells were transiently transfected with an NFAT-luc reporter plasmid, treated with MβCD for 40 min, washed, stimulated with OKT3 or PMA plus ionomycin (P+I) in conditioned culture medium without FCS for 6 h, and then tested for NFAT activity by NFAT reporter assay. (D) After LAT-GFP transfectants were pretreated for 40 min with 4 mM MβCD, the cells were stimulated with poly-L-lysine beads or anti-CD3 beads for 20 min in the presence of 4 mM MβCD. Conjugates were fixed with formaldehyde and observed by confocal microscopy. (E) A selected area (2-μm square) on the LAT-GFP patches in LAT-GFP transfectants treated with or without MβCD was photobleached, and fluorescence recovery was monitored. (F) Bleaching recovery kinetics is represented as the percentage of FRAP for LAT-GFP in patches in the presence or absence of MβCD. Data are representative of three individual experiments.

cant difference in the frequency of patch formation between MβCD-treated cells and cells without treatment (Fig. 6 D). This result indicates that successful activation

of early signaling pathways in MβCD-treated cells appears to be sufficient to induce LAT-GFP patch formation. However, when FRAP was performed to assess the mobility of LAT-GFP under MβCD treatment, we observed a striking effect for cholesterol depletion. As shown in Fig. 6 E, LAT-GFP localized in patches from MβCD-treated cells recovered very quickly after photobleaching, whereas that from nontreated cells demonstrated a limited recovery as before (Fig. 4 A). For both MβCD-treated and non-treated cells, LAT-GFP fluorescence returned to maximal levels within 1 min. However, whereas the recovery was only 20% in nontreated cells, this percentage increased to 50% in MβCD-treated cells (Fig. 6 F). Thus, MβCD treatment clearly induced an increase in the mobility of molecules in LAT-GFP patches. These results suggest that when cholesterol is removed from the cell, raft structure is altered, resulting in the inability of LAT that usually aggregates and resides in aggregated rafts to remain in the same position. The correlation between the increased mobility of LAT-GFP and the inhibition of NFAT activity (Fig. 6 C) indicates the importance of LAT mobility in aggregated rafts for T cell activation.

The role of the cytoplasmic domain of LAT in the mobility of LAT in aggregated rafts

The cytoplasmic domain of LAT has previously been reported to be essential for the interaction of LAT with other signaling molecules (Zhang et al., 2000). To investigate whether LAT-GFP patch formation after TCR stimulation is dependent on the cytoplasmic domain of LAT, and hence, interactions between LAT and other signaling molecules, Jurkat-derived transfectants expressing a fusion protein consisting of the 36 amino acid NH$_2$-terminal transmembrane domain of LAT fused to GFP, LAT(TM)-GFP, were established. Although this fusion protein contains the two Cys residues required for LAT palmitoylation, it does not contain multiple tyrosine residues that are indispensable for interaction with other proteins. After stimulation by anti-CD3–coated beads, LAT(TM)-GFP transfectants were observed by confocal microscopy and scored for patch formation. The extent of patch formation at the cell–bead interface in LAT(TM)-GFP transfectants was comparable to that in LAT-GFP transfectants (Fig. 7, A and B). Moreover, the size of patches was similar in both LAT- and LAT(TM)-GFP transfectants. Thus, these results clearly demonstrate that the presence of transmembrane domain of LAT is sufficient for accumulation of LAT into aggregated rafts in response to TCR stimulation.

Next, we investigated whether the cytoplasmic domain of LAT is required for the reduction in LAT mobility seen after TCR stimulation. LAT(TM)-GFP transfectants were stimulated with anti-CD3–coated beads, and photobleaching was performed on regions of patch formation. Compared with LAT-GFP, the recovery after bleaching was considerably greater in LAT(TM)-GFP transfectants (Fig. 7 C). The fluorescence recovery was reached 40% of total fluorescence 1 min after bleaching, and remained at this percentage during a 5-min time course (Fig. 7 D). Thus, the cytoplasmic domain of LAT is important for the reduction in the mobility of LAT at areas of patch formation.
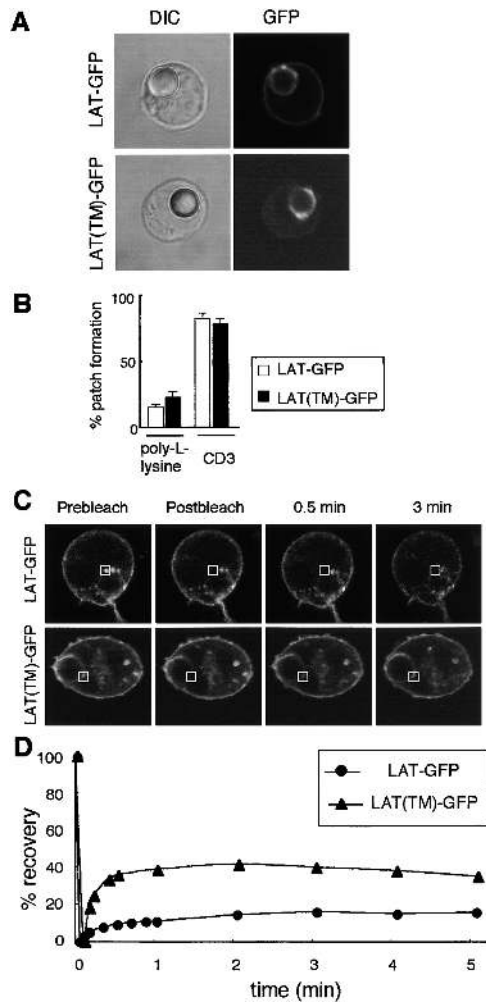
Figure 7. The mobility of LAT(TM)-GFP in patches after TCR stimulation. Jurkat-derived transfectants expressing LAT-GFP or LAT(TM)-GFP were mixed with anti-CD3 beads for 20 min. (A) Conjugates were fixed with formaldehyde and observed by confocal microscopy. In the left column are differential interference contrast (DIC) images, and in the left column are LAT-GFP fluorescence images. LAT-GFP and LAT(TM)-GFP patches were observed at the contact site between the cell and the bead. (B) Each column represents the average of at least three individual experiments in which more than 100 conjugates were scored for patch formation. (C) A selected area (2-μm square) on the LAT/GFP or LAT(TM)-GFP patches was photobleached, and fluorescence recovery was monitored. Images at representative time points are shown. (D) Bleaching recovery kinetics is represented as the percentage of FRAP for LAT-GFP and LAT(TM)-GFP in patches. Data are representative of five individual experiments.

The PLCγ1 binding site in LAT is important for the reduced mobility of LAT in aggregated rafts

After TCR engagement, LAT is tyrosine-phosphorylated by ZAP-70, creating docking sites for multiple downstream effector proteins. It has been shown that the distal four tyrosine residues of LAT bind PLCγ1, Grb2, and Gads, and these interactions are essential for TCR signal transduction (Zhang et al., 2000; Sommers et al., 2001). Next, we wanted to determine which molecular interactions influence LAT mobility in aggregated rafts. We established the following Jurkat-derived transfectants expressing different LAT-GFP

mutants containing substitutions of critical tyrosines with phenylalanines in the LAT cytoplasmic domain (Fig. 8 A): LAT(Y136F)-GFP with a mutation at Tyr^{136}, a site for PLCγ1 binding; LAT(3YF)-GFP with mutations at Tyr^{175}, Tyr^{195}, and Tyr^{235}, sites for Grb2/Gads binding; and LAT(4YF)-GFP with mutations at the above four tyrosine residues that abolish both PLCγ1- and Grb2/Gads-binding. To confirm the association of LAT-GFP with PLCγ1 or Grb2, we activated the transfectants with OKT3, immunoprecipitated PLCγ1, or Grb2 with specific antibodies, and detected LAT-GFP association by anti-GFP blotting (Fig. 8 B). Although PLCγ1 and Grb2 were clearly associated with LAT-GFP in the wild-type LAT-GFP transfectant, mutations of the distal four tyrosines in the LAT(4YF)-GFP transfectant completely abolished these interactions. As expected, a mutation at Tyr^{136} abrogated PLCγ1 binding with LAT, but not Grb2 binding. In the LAT(3YF)-GFP mutant, the association of Grb2 with LAT was almost absent, and that of PLCγ1 with LAT was also undetectable (unpublished data). This is consistent with previous findings (Zhang et al., 2000), and we did not further analyze the LAT(3YF)-GFP transfectant because it was impossible to distinguish LAT(3YF)-GFP from LAT(4YF)-GFP in terms of protein interactions.

Using the above LAT-GFP mutants, we performed FRAP experiments to assess effects of protein interactions on LAT mobility. The extent of patch formation in response to anti-CD3–coated bead stimulation was comparable between LAT-GFP, LAT(Y136F)-GFP, and LAT(4YF)-GFP transfectants (unpublished data). In contrast to the low recovery of LAT-GFP fluorescence after photobleaching in LAT-GFP transfectants, the recovery of LAT(4YF)-GFP was considerably higher. Moreover, improved fluorescence recovery was also observed in LAT(Y136F)-GFP transfectants (Fig. 8, C and D). These results indicate that LAT localizes to aggregated rafts in a stable manner by way of protein interactions; especially PLCγ1 binding.

Discussion

Analysis using live LAT-GFP transfectants revealed that LAT-GFP is homogeneously distributed throughout the plasma membrane (Figs. 4–8). Patches were rarely visible at the plasma membrane, suggesting that in lymphocytes, rafts do not exist in large size. However, when these cells were stimulated with anti-CD3–coated beads, rafts aggregated and patches were formed around the circumference of the beads. This patch formation was specifically dependent on TCR stimulation, and could not be induced by stimulation with beads conjugated to anti-CD28 antibodies or antibodies against adhesion molecules. Consistent with our results, it has been reported that when Jurkat cells are stimulated with anti-CD3–coated beads, LAT accumulates at the bead–cell contact area, and microtubule-organizing center reorientation and actin polymerization are observed toward the bead attachment site (Lowin-Kropf et al., 1998; Harder and Kuhn, 2000). In contrast, Viola et al. (1999) have reported that although formation of a dense cap (raft capping) can be induced in the zone of contact when human resting T cells are stimulated with beads coated with both anti-CD3 and
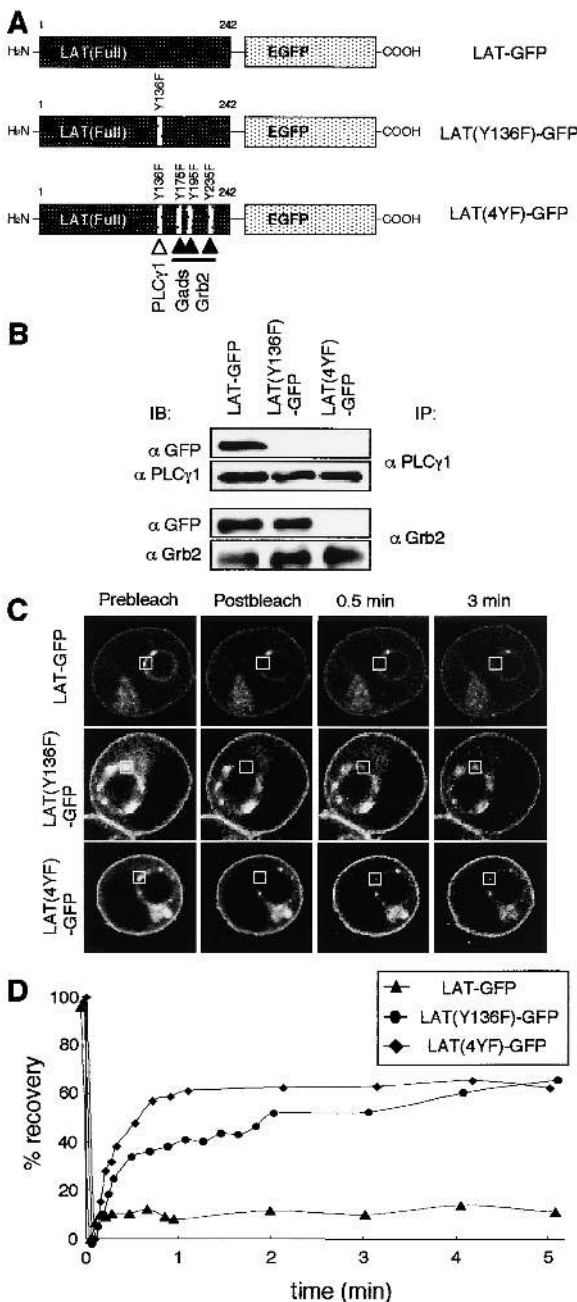
Figure 8. The PLCγ1 binding site of LAT is important for the reduced mobility of LAT in aggregated rafts. (A) Schematic representations of the LAT-GFP, LAT(Y136F)-GFP, and LAT(4YF)-GFP fusion proteins. A LAT-GFP chimera was constructed by attaching EGFP to the full length of mouse LAT. Y136 is a binding site for PLCγ1, and Y175, Y195, and Y235 are binding sites for Grb2/Gads in mouse LAT. Mutated amino acids are shown for each construct. (B) Association of LAT-GFP with PLCγ1 or Grb2. The LAT-GFP, LAT(Y136F)-GFP, and LAT(4YF)-GFP transfectants were stimulated with OKT3 for 5 min. Cell lysates were immunoprecipitated with either anti-PLCγ1 or anti-Grb2 antibody, and immunoprecipitates were analyzed by immunoblotting with anti-GFP and antibodies specific for the immunoprecipitated protein. (C) After the LAT-GFP, LAT(Y136F)-GFP, and LAT(4YF)-GFP transfectants were mixed with anti-CD3 beads for 20 min, a selected area (2-μm square) on the patches was photobleached, and fluorescence recovery was monitored. Images at representative time points are shown. (D) Bleaching recovery kinetics is represented as the percentage of FRAP in patches. Data are representative of three individual experiments.

anti-CD28 antibodies, stimulation for these cells with anti-CD3–coated beads alone is not able to induce raft aggregation. Thus, it is conceivable that depending on the cell type used, there are different requirements for raft aggregation and cytoskeletal changes. Indeed, we observed that the efficiency of LAT-GFP patch formation was different in mouse-activated T cells stimulated with anti-TCR–coated beads or beads coated with anti-TCR plus anti-CD28 (Fig. 5 B). In contrast to the data using resting T cells reported earlier (Viola et al., 1999), we were not able to detect raft capping in primary activated T cells stimulated with anti-TCR– and anti-CD28–coated beads.

Although molecules involved in raft aggregation have been reported (Krawczyk et al., 2000), the mechanism for activation-dependent raft aggregation remains obscure. However, several possibilities can be envisioned for this. First, although raft-associated receptors could be separated in different small rafts before activation, receptor oligomerization could be induced by ligand-mediated cross-linking, which results in coalescence of small rafts into a larger domain. Cross-linking of the Fcε receptor with IgE plus antigen has been shown to trigger aggregation of DiI, a fluorescent probe thought to partition into rafts (Thomas et al., 1994). A second mechanism by which raft aggregation could be promoted is by increasing affinity for rafts of a protein that does not reside in rafts before stimulation. After an activation-dependent change in its affinity, the protein accumulates in rafts and induces coalescence of small raft domains by way of interaction with other raft-associated proteins. Lipid modification such as palmitoylation is one mechanism that can increase the affinity of a given protein to rafts. Finally, a specific molecule such as agrin, an extracellular proteoglycan, could be primarily responsible for raft aggregation (Khan et al., 2001). The activated, deglycosylated form of agrin can be produced by activated T cells and has been shown to drive raft clustering presumably due to its lectin-like capacity. The molecular mechanisms by which the signal from the TCR induces raft aggregation are still unknown. Because the above mechanisms are not mutually exclusive, combined machinery may be operative to induce raft aggregation in T cells.

The data derived using the photobleaching techniques clearly demonstrated that LAT associated with aggregated rafts becomes less mobile and does not exchange with LAT in the plasma membrane outside aggregated rafts. This result can be explained by several possibilities. In response to raft aggregation, raft-associated lipids and proteins might be strongly packed in the plasma membrane, which leads to the inhibition of their mobility. Moreover, because a variety of signal transduction molecules are known to be recruited to rafts after TCR stimulation, protein–protein or protein–lipid interactions that are actively promoted in aggregated rafts may also act as an impediment to the mobility of raft-localized molecules. Indeed, the mobility of LAT(TM)-GFP and LAT(4YF)-GFP in patches was considerably higher compared with that of LAT-GFP (Figs. 7 and 8). This suggests that protein–protein interactions mediated through the cytoplasmic domain of LAT have a great influence on LAT mobility. Consistent with our observation, Harder and Kuhn have demonstrated that LAT/TCR assemblies are important

to form a structural scaffold for TCR signal transduction proteins using a novel method to immunoisolate plasma membrane subfragments (Harder and Kuhn, 2000). With regard to associated proteins that mainly affect LAT mobility, we demonstrated that the PLCγ1 binding site in LAT is critical for LAT dynamics in membrane rafts after TCR stimulation (Fig. 8, C and D). The mechanism for a specific role of PLCγ1 over other associated proteins in LAT mobility remains to be determined, but the existence of an NH$_2$-terminal pleckstrin homology domain in PLCγ1, which is known to contribute the association of PLCγ1 with the plasma membrane, could affect LAT mobility in aggregated rafts.

In addition to protein–protein interactions, raft structure supported by membrane cholesterol appears to be important for maintaining LAT mobility in aggregated rafts. Because extraction with 10 mM MβCD impairs Jurkat cells irreversibly, we treated Jurkat cells and LAT-GFP transfectants with 4 mM MβCD for 40 min to induce cholesterol depletion. It was reported that signaling proteins accumulated in TCR-enriched immunoisolates and the amounts of LAT and Lck in the raft fractions were both clearly reduced in cells treated with the same concentration of MβCD (Harder and Kuhn, 2000). Furthermore, they demonstrated that signal transduction such as tyrosine phosphorylation of cellular proteins was inhibited with this treatment. In contrast to their data, we could not observe an inhibition of tyrosine phosphorylation of cellular proteins (Fig. 6 B) or of Ca^{2+} response (unpublished data) by this treatment. Successful activation of early signaling events under this MβCD treatment may lead to efficient patch formation of LAT-GFP (Fig. 6 D). Therefore, it is possible that the initial process of raft aggregation on stimulation is relatively resistant to cholesterol depletion. However, raft structure at the area of raft aggregation has been changed by this treatment because it was found that the mobility of LAT-GFP in patches markedly increased (Fig. 6, E and F). Intriguingly, in association with the increased mobility of LAT-GFP, NFAT transcriptional activity was significantly impaired in cells treated with 4 mM MβCD (Fig. 6 C). Thus, disruption of raft structure may impair the stability of raft-associated proteins in aggregated rafts, resulting in the inhibition of protein–protein interactions necessary for TCR-mediated signal transduction. Because initial signaling events were not impaired, we believe that the increased mobility of LAT-GFP is not a secondary consequence of the inhibition of protein–protein interactions for TCR signaling by MβCD treatment, but is directly related to the changes of raft structure. The results also imply that raft organization and the decreased mobility of LAT in aggregated rafts should be maintained during the progression of signaling events at the plasma membrane.

Another factor that affects the mobility of raft-localized proteins could be cytoskeletal reorganization associated with raft clustering (Bunnell et al., 2001; Miceli et al., 2001). It has already been shown that raft patches formed by crosslinking of glycosylphosphatidylinositol-anchored proteins and GM1 accumulate F-actin in Jurkat cells (Harder and Simons, 1999). We have also observed in this work that F-actin was colocalized with LAT-GFP patches (Fig. 3). It is not surprising that molecules in aggregated rafts with cyto-

skeletally associated structures could be restricted in their mobility compared with those in other areas of the plasma membrane. Whatever the mechanism by which LAT mobility is decreased after raft aggregation, further experiments using raft-associated proteins other than LAT appear to be necessary to confirm whether our findings elucidate a generalized feature for proteins in aggregated rafts. Moreover, although we have focused on raft-localized proteins in this study, it is also important to investigate whether lipids that constitute rafts exhibit the same characteristics as these proteins.

In this analysis, we used a raft-localized protein (LAT) to provide the first report of the dynamics of rafts in live T cells. We believe the assay system described in this report will be highly useful for the analysis of molecular interactions in rafts on T cells in the future. We also anticipate that highly evolved systems, such as spatio-temporal investigation using FRET-based sensors, will supply an even more detailed view of the change in mobility of molecules accumulated in rafts and the molecular interactions between different molecules in aggregated rafts during T cell activation.

Materials and methods

DNA construction

A DNA fragment coding for the full-length murine LAT (Zhang et al., 1998a) was obtained by RT-PCR using the 2B4 T cell hybridoma cDNA (Samelson et al., 1983) as a template. The sense and the antisense primers contained restriction sites for XhoI and for BamHI, respectively. The fragment was subcloned into pPCR-Script® (Stratagene) and was sequenced. A DNA fragment coding for EGFP was obtained from pEGFP-N1 vector (CLONTECH Laboratories, Inc.). The XhoI/BamHI fragment from pPCR-Script® containing full-length LAT and the BamHI/NotI fragment from pEGFP-N1 were then subcloned into the XhoI/NotI site of pMKIT Neo, an SRα promoter–driven expression vector (provided by Dr. K. Maruyama, Tokyo Medical and Dental University, Tokyo, Japan), and sequenced to check the junctional sequence. The predicted molecular mass of the LAT-GFP fusion protein is ~65 kD. A LAT(TM)-GFP chimera was constructed by replacing the full-length LAT with the 36 NH$_2$-terminal amino acids in LAT. The LAT(Y136F)-GFP and LAT(4YF)-GFP mutants were generated from the wild-type LAT-GFP cDNA in pMKIT Neo vector using the Stratagene QuikChange® kit.

Cell culture and transfection

Jurkat cells were cultured in RPMI 1640 medium supplemented with 10% FCS, 50 μM 2-mercaptoethanol, 2 mM L-glutamine, and antibiotics. Jurkat-derived stable transfectants were established as described previously (Saitoh et al., 1995). Growing colonies after transfection were expanded in selective media supplemented with G418 (GIBCO BRL) at 1 mg/ml and assayed for LAT-GFP expression by fluorescence microscopy. Clones that express LAT-GFP at a high level, as analyzed by flow cytometry, were selected for further study. We also confirmed a similar level of TCR expression in our LAT-GFP transfectants as compared with Jurkat cells.

Retroviral-mediated gene transfer

LAT-GFP was cloned into the pMX-puro retroviral vector (Onishi et al., 1998). Plat-E cells (6 × 10^5 cells per well), the potent retrovirus-packaging cell line derived from 293T cells (Morita et al., 2000), were plated into a 6-well plate, incubated for 24 h, and then transfected with 1 μg of the pMX-puro–harboring LAT-GFP in conjunction with 3 μl FuGENE™ (Roche Diagnostics) according to the manufacturer's recommendation. 24 h after transfection, the culture medium was replaced with fresh medium (10% FCS/RPMI 1640), the cells were continued to be cultured for another 24 h, and the virus-containing medium was collected and filtered. Purified C57BL/6 T cells were activated with 2C11 and PV-1 and were infected after 36 h using a 1:2 volume of viral supernatant and polybrene (Sigma-Aldrich) at 4 μg /ml, centrifuged at 2,500 rpm for 90 min at 30°C, and incubated at 37°C for 6 h before being supplied with fresh media with IL-2 (37.5 U/ml) and expanded until day 5 after primary activation.

Antibodies and reagents

The following antibodies were used: OKT3 (American Type Culture Collection), anti-CD3ε mAb; CLB-402 (CALTAG Laboratories), anti-CD28 mAb; MEM-25 (CALTAG Laboratories), anti-LFA-1 mAb; IM7.8.1 (CEDAR-LANE Laboratories Limited), anti-CD44 mAb; anti-LAT pAb (Upstate Biotechnology); BRA-10G (Cymbus Biotechnology Ltd.), biotin-conjugated anti-CD59 antibody; BHPT-1 (Exalpha Biologicals), biotin-conjugated anti-CD45 antibody; DFT-1 (Cosmo Bio Co.) biotin-conjugated anti-CD43 mAb; MOL171 (Kosugi et al., 2001), biotin-conjugated anti-Lck mAb; PY20 (Transduction Laboratories), anti-phosphotyrosine mAb; anti-PLCγ1 mAb (Upstate Biotechnology); sc-255 (Santa Cruz Biotechnology, Inc.), anti-Grb2 pAb; and anti-GFP pAb (Medical & Biological Laboratories Co., Ltd.). The antibodies against mouse surface antigens are as follows: 2C11 (BD Biosciences), anti-CD3ε mAb; H57–597 (BD Biosciences), anti-TCRβ mAb; and PV-1 (Southern Biotechnology Associates, Inc.), anti-CD28 mAb. MβCD, poly-L-lysine, phalloidin-TRITC, and biotin-conjugated CTx-B were purchased from Sigma-Aldrich. Polystylene latex microspheres and streptavidin-Texas red (SA-TR) were purchased from Polysciences, Inc. and Molecular Probes, Inc., respectively.

Stimulation of cells with antibody-coated beads and confocal microscopy

Antibodies were absorbed to 6-μm-diam latex beads as described previously (Lowin-Kropf et al., 1998). In brief, 10 μg of purified antibody were mixed with 10^7 polystyrene beads in a final volume of 1 ml PBS, and incubated for 90 min at RT with constant tumbling. Beads were then blocked in 1.5 ml PBS/1% BSA for 30 min. After three washes in PBS, latex beads were resuspended in PBS and stored at 4°C. Efficient antibody absorption was verified by flow cytometry. LAT-GFP transfectants (2×10^5) were mixed with antibody-coated beads (10^5) for 20 min at 37°C. We stimulated cells for 20 min unless otherwise specified (Fig. 2 C). The cell–bead mixture was then fixed for 10 min in PBS/3.7% formaldehyde, and samples were mounted on slides and viewed under a confocal microscope. In some experiments, cells were incubated with either 1–10 μg/ml biotin-conjugated antibodies or 5 μg/ml biotin-conjugated CTx-B, followed by 10 μg/ml SA-TR. LAT-GFP patch formation was scored as positive if at least one distinct patch was observed at the bead contact area. We counted more than 100 cells that incorporated or were in contact with beads, and calculated the percentage of the patch formation. Confocal microscopy was performed with a 63×/1.4 oil objective lens on a confocal microscope (model LSM 510; Carl Zeiss MicroImaging, Inc.), using laser excitation at 488 and 543 nm. The widths of GFP and Texas red emission channels were set such that bleed-through across channels was negligible.

FRAP experiments

After LAT-GFP transfectants were mixed with anti-CD3 beads, conjugates were placed on slides in culture medium (10% FCS/RPMI 1640 without phenol red and 25 mM Hepes) that was prewarmed at 37°C without fixation. A selected area (2-μm square) on the LAT/GFP patches was photobleached for 3–5 s by 488 nm laser at 18 mW. Pre- and postbleach images were collected periodically until fluorescence was recovered at a plateau level, and the fluorescence intensity in the photobleached area of each image was measured. The postbleach intensity was corrected for overall loss of fluorescence determined from total fluorescence in the whole-cell images taken at the beginning and end of the experiment. Bleaching recovery kinetics is represented as the percentage of FRAP (Spector et al., 1997). The corrected pre- and postbleach intensities are normalized to 100 and 0%, respectively. During FRAP experiments described above, we did not strictly control the temperature of medium in which cell–bead conjugates were suspended using a heated stage. However, we did not observe any difference between the results of FRAP experiments with or without using a heated stage.

MβCD treatment

Jurkat cells were pretreated with 4 mM MβCD for 40 min at 37°C. After washing, the cells were stimulated with OKT3, and tyrosine phosphorylation of cellular proteins was analyzed as described previously (Kosugi et al., 2001). For NFAT-luc reporter assays, Jurkat cells (5×10^5) were transfected with 500 ng of NFAT-luc and 50 ng of pRL-TK using DMRIE-C (GIBCO BRL). One day after transfection, cells were treated with 4 mM MβCD for 40 min, washed, and then stimulated with 1 μg/ml immobilized OKT3, or 1 μM ionomycin plus 50 ng/ml PMA for 6 h in conditioned medium that did not contain FCS. As conditioned medium, we used RPMI 1640 with twofold Insulin-Transferrin-Selenium-S Supplement (GIBCO BRL). For LAT-GFP patch formation and FRAP experiments, LAT-GFP transfectants were pretreated with 4 mM MβCD for 40 min at 37°C, and stimulated with anti-CD3–coated beads in the presence of MβCD.

Lipid analysis

Cells (10^7) were collected, washed twice with PBS, and the lipids were extracted from the cell pellets as described previously (Inokuchi et al., 2000). Lipids were separated by HPTLC and were visualized with 3% cupric acetate/8% phosphoric acid.

Isolation of a raft fraction, immunoprecipitation, and immunoblotting analysis

Isolation of a raft fraction, immunoprecipitation, and immunoblotting analysis were performed as described previously (Kosugi et al., 2001).

References

Allenspach, E.J., P. Cullinan, J. Tong, Q. Tang, A.G. Tesciuba, J.L. Cannon, S.M. Takahashi, R. Morgan, J.K. Burkhardt, and A.I. Sperling. 2001. ERM-dependent movement of CD43 defines a novel protein complex distal to the immunological synapse. *Immunity.* 15:739–750.

Boerth, N.J., J.J. Sadler, D.E. Bauer, J.L. Clements, S.M. Gheith, and G.A. Koretzky. 2000. Recruitment of SLP-76 to the membrane and glycolipid-enriched membrane microdomains replaces the requirement for linker for activation of T cells in T cell receptor signaling. *J. Exp. Med.* 192:1047–1058.

Bunnell, S.C., V. Kapoor, R.P. Trible, W. Zhang, and L.E. Samelson. 2001. Dynamic actin polymerization drives T cell receptor-induced spreading: a role for the signal transduction adaptor LAT. *Immunity.* 14:315–329.

Cherukuri, A., M. Dykstra, and S.K. Pierce. 2001. Floating the raft hypothesis: Lipid raft play a role in immune cell activation. *Immunity.* 14:657–660.

Finco, T.S., T. Kadlecek, W. Zang, L.E. Samelson, and A. Weiss. 1998. LAT is required for TCR-mediated activation of PLCγ1 and the Ras pathway. *Immunity.* 9:617–626.

Harder, T., and K. Simons. 1999. Clusters of glycolipid and glycosylphosphatidyl-inositol-anchored proteins in lymphoid cells: accumulation of actin regulated by local tyrosine phosphorylation. *Eur. J. Immunol.* 29:556–562.

Harder, T., and M. Kuhn. 2000. Selective accumulation of raft-associated membrane protein LAT in T cell receptor signaling assemblies. *J. Cell Biol.* 151:199–207.

Inokuchi, J.-I., S. Uemura, K. Kabayama, and Y. Igarashi. 2000. Glycosphingolipid deficiency affects functional microdomain formation in Lewis lung carcinoma cells. *Glycoconj. J.* 17:239–245.

Janes, P.W., S.C. Ley, and A.I. Magee. 1999. Aggregation of lipid rafts accompanies signaling via the T cell antigen receptor. *J. Cell Biol.* 147:447–461.

Janes, P.W., S.C. Ley, A.I. Magee, and P.S. Kabouridis. 2000. The role of lipid rafts in T cell antigen receptor (TCR) signaling. *Semin. Immunol.* 12:23–34.

Khan, A.A., C. Bose, L.S. Yam, M.J. Soloski, and F. Rupp. 2001. Physiological regulation of the immunological synapse by agrin. *Science.* 292:1681–1686.

Klein, U., G. Gimpl, and F. Fahrenholz. 1995. Alteration of the myometrial plasma membrane cholesterol content with β-cyclodextrin modulates the binding affinity of the oxytocin receptor. *Biochemistry.* 34:13784–13793.

Kosugi, A., J. Sakakura, K. Yasuda, M. Ogata, and T. Hamaoka. 2001. Involvement of SHP-1 tyrosine phosphatase in TCR-mediated signaling pathways in lipid rafts. *Immunity.* 14:669–680.

Krawczyk, C., B. Bachmaier, T. Sasaki, R.G. Jones, S.B. Snapper, D. Bouchard, I. Kozieradzki, P.S. Ohashi, F.W. Alt, and J.M. Penninger. 2000. Cbl-b is a negative regulator of receptor clustering and raft aggregation in T cells. *Immunity.* 13:463–473.

Lowin-Kropf, B., V.S. Shapiro, and A. Weiss. 1998. Cytoskeletal polarization of T cells is regulated by an immunoreceptor tyrosine-based activation motif-dependent mechanism. *J. Cell Biol.* 140:861–871.

Miceli, M.C., M. Moran, C.D. Chung, V.P. Patel, T. Low, and W. Zinnanti. 2001. Co-stimulation and counter-stimulation: lipid raft clustering controls TCR signaling and functional outcomes. *Semin. Immunol.* 13:115–128.

Montixi, C., C. Langlet, A.-M. Bernard, J. Thimonier, C. Dubois, M.-A. Wurbel, J.-P. Chauvin, M. Pierres, and H.-T. He. 1998. Engagement of T cell receptor triggers its recruitment to low-density detergent-insoluble membrane domains. *EMBO J.* 17:5334–5348.

Moran, M., and M.C. Miceli. 1998. Engagement of GPI-linked CD48 contributes to TCR signals and cytoskeletal reorganization: a role for lipid rafts in T cell activation. *Immunity.* 9:787–796.

Morita, S., T. Kojima, and T. Kitamura. 2000. Plat-E: an efficient and stable system for transient packaging of retroviruses. *Gene Ther.* 7:1063–1066.

Onishi, M., T. Nosaka, K. Misawa, A.L.F. Mui, D. Gorman, M. McMahon, A. Miyajima, and T. Kitamura. 1998. Identification and characterization of a constitutively active STAT5 mutant that promotes cell proliferation. *Mol. Cell. Biol.* 18:3871–3879.

Rodgers, W., and J.K. Rose. 1996. Exclusion of CD45 inhibits activity of p56^{lck} associated with glycolipid-enriched membrane domains. *J. Cell Biol.* 135: 1515–1523.

Saitoh, S.-I., A. Kosugi, S. Noda, N. Yamamoto, M. Ogata, Y. Minami, K. Miyake, and T. Hamaoka. 1995. Modulation of T cell receptor-mediated signaling pathway by thymic shared antigen-1 (TSA-1)/stem cell antigen-2 (Sca-2). *J. Immunol.* 155:5574–5581.

Samelson, L.E., R.N. Germain, and R.H. Schwartz. 1983. Monoclonal antibodies against the antigen receptor on a cloned T-cell hybrid. *Proc. Natl. Acad. Sci. USA.* 80:6972–6976.

Shan, X., and R.L. Wange. 1999. Itk/Emt/Tsk activation in response to CD3 cross-linking in Jurkat T cells requires ZAP-70 and Lat and is independent of membrane recruitment. *J. Biol. Chem.* 274:29323–29330.

Simons, K., and E. Ikonen. 1997. Functional rafts in cell membranes. *Nature.* 387: 569–572.

Sommers, C.L., R.K. Menon, A. Grinberg, W. Zhang, L.E. Samelson, and P.E. Love. 2001. Knock-in mutation of the distal four tyrosines of linker for activation of T cells blocks murine T cell development. *J. Exp. Med.* 194:135–142.

Spector, D.L., R.D. Goldman, and L.A. Leinwand. 1997. Fluorescence photobleaching techniques. *In* Cells: A Laboratory Manual. Cold Spring Harbor Laboratory, Cold Spring Harbor, New York. 79.1–79.23.

Thomas, J.L., D. Holowka, B. Baird, and W.W. Webb. 1994. Large-scale co-aggregation of fluorescent lipid probes with cell surface proteins. *J. Cell Biol.* 125:795–802.

van der Goot, F.G., and T. Harder. 2001. Raft membrane domains: from a liquid-ordered membrane phase to a site of pathogen attack. *Semin. Immunol.* 13: 89–97.

Varma, R., and S. Mayor. 1998. GPI-anchored proteins are organized in submicron domains at the cell surface. *Nature.* 394:798–801.

Viola, A., S. Schroeder, Y. Sakakibara, and A. Lanzavecchia. 1999. T lymphocyte costimulation mediated by reorganization of membrane microdomains. *Science.* 283:680–682.

Wange, R.L., and L.E. Samelson. 1996. Complex complexes: signaling at the TCR. *Immunity.* 5:197–205.

Weiss, A., and D.R. Littman. 1994. Signal transduction by lymphocyte antigen receptors. *Cell.* 76:263–274.

Xavier, R., T. Brennan, Q. Li, C. McCormack, and B. Seed. 1998. Membrane compartmentation is required for efficient T cell activation. *Immunity.* 8:723–732.

Zhang, W., J. Sloan-Lancaster, J. Kitchen, R.P. Trible, and L.E. Samelson. 1998a. LAT: the ZAP-70 tyrosine kinase substrate that links T cell receptor to cellular activation. *Cell.* 92:83–92.

Zhang, W., R.P. Trible, and L.E. Samelson. 1998b. LAT palmitoylation: its essential role in membrane microdomain targeting and tyrosine phosphorylation during T cell activation. *Immunity.* 9:239–246.

Zhang, W., B.J. Irvin, R.P. Trible, R.T. Abraham, and L.E. Samelson. 1999. Functional analysis of LAT in TCR-mediated signaling pathways using a LAT-deficient Jurkat cell line. *Int. Immunol.* 11:943–950.

Zhang, W., R.P. Trible, M. Zhu, S.K. Liu, C.J. McGlade, and L.E. Samelson. 2000. Association of Grb2, Gads, and phospholipase C-γ1 with phosphorylated LAT tyrosine residues. Effect of LAT tyrosine mutations on T cell antigen-receptor-mediated signaling. *J. Biol. Chem.* 275:23355–23361.